

Activation of ventral tegmental area dopaminergic neurons reverses pathological allodynia resulting from nerve injury or bone cancer

Molecular Pain
Volume 14: 1–11
© The Author(s) 2018
Reprints and permissions:
sagepub.com/journalsPermissions.nav
DOI: 10.1177/1744806918756406
journals.sagepub.com/home/mpx


Moe Watanabe¹, Michiko Narita¹, Yusuke Hamada¹, Akira Yamashita¹, Hideki Tamura², Daigo Ikegami^{1,3}, Takashige Kondo¹, Tatsuto Shinzato¹, Takatsune Shimizu⁴, Yumi Fukuchi⁴, Akihiro Muto⁴, Hideyuki Okano^{2,5}, Akihiro Yamanaka⁶, Vivianne L Tawfik⁷, Naoko Kuzumaki¹, Edita Navratilova³, Frank Porreca³ and Minoru Narita^{1,2}

Abstract

Chronic pain induced by nerve damage due to trauma or invasion of cancer to the bone elicits severe ongoing pain as well as hyperalgesia and allodynia likely reflecting adaptive changes within central circuits that amplify nociceptive signals. The present study explored the possible contribution of the mesolimbic dopaminergic circuit in promoting allodynia related to neuropathic and cancer pain. Mice with ligation of the sciatic nerve or treated with intrafemoral osteosarcoma cells showed allodynia to a thermal stimulus applied to the paw on the injured side. Patch clamp electrophysiology revealed that the intrinsic neuronal excitability of ventral tegmental area (VTA) dopamine neurons projecting to the nucleus accumbens (N.Acc.) was significantly reduced in those mice. We used tyrosine hydroxylase (TH)-cre mice that were microinjected with adeno-associated virus (AAV) to express channelrhodopsin-2 (ChR2) to allow optogenetic stimulation of VTA dopaminergic neurons in the VTA or in their N.Acc. terminals. Optogenetic activation of these cells produced a significant but transient anti-allodynic effect in nerve injured or tumor-bearing mice without increasing response thresholds to thermal stimulation in sham-operated animals. Suppressed activity of mesolimbic dopaminergic neurons is likely to contribute to decreased inhibition of N.Acc. output neurons and to neuropathic or cancer pain-induced allodynia suggesting strategies for modulation of pathological pain states.

Keywords

Neuropathic pain, cancer pain, dopamine, mesolimbic dopaminergic neurons, optogenetics

Date Received: 14 November 2017; revised 3 December 2017; accepted: 13 December 2017

¹Department of Pharmacology, Hoshi University School of Pharmacy and Pharmaceutical Sciences, Shinagawa-ku, Tokyo, Japan

²Life Science Tokyo Advanced Research Center (L-StaR), Hoshi University School of Pharmacy and Pharmaceutical Sciences, Shinagawa-ku, Tokyo, Japan

³Department of Pharmacology, Arizona Health Sciences Center, University of Arizona, Tucson, AZ, USA

⁴Department of Pathophysiology, Hoshi University School of Pharmacy and Pharmaceutical Sciences, Shinagawa-ku, Tokyo, Japan

⁵Department of Physiology, Keio University School of Medicine, Shinjuku-ku, Tokyo, Japan

⁶Department of Neuroscience II, Research Institute of Environmental Medicine, Nagoya University, Furo-cho, Chikusa-ku, Nagoya, Japan

⁷Department of Anesthesiology, Perioperative and Pain Medicine, Stanford University School of Medicine, Palo Alto, CA, USA

Corresponding Author:

Minoru Narita, Department of Pharmacology, Hoshi University School of Pharmacy and Pharmaceutical Sciences, 2-4-41 Ebara, Shinagawa-ku, Tokyo 142-8501, Japan.

Email: narita@hoshi.ac.jp



Introduction

Substantial evidence has implicated the mesolimbic dopaminergic reward valuation pathway in both acute and chronic pain states. Pain and pain relief are salient stimuli that produce motivation for protective or escape behaviors that promote safety.¹ Chronic pain conditions are accompanied by adaptive changes within central circuits that amplify the consequences of sensory inputs. How chronic pain influences central reward pathways, including the mesolimbic dopaminergic system, is poorly understood.

Neuropathic pain results from damage or dysfunction of nerves and is chronic and debilitating, often characterized by ongoing pain as well as hyperalgesia and allodynia. Bone cancer pain has been suggested to result from contributions of structural, inflammatory, and neuropathic components that promote ongoing pain, breakthrough pain, and evoked hypersensitivity to normally innocuous stimuli. These conditions are poorly managed with current therapies largely ineffective in many patients. Both ongoing pain and allodynia are important clinical conditions that represent an important unmet medical need and are devastating to the quality of life of patients.

In the present study, we hypothesized that neuropathic or bone cancer pain would produce pronociceptive adaptive changes in mesolimbic dopaminergic neurons. We used electrophysiological, neurochemical, optogenetic, and behavioral techniques to demonstrate that increased dopamine release in the nucleus accumbens (N.Acc.) resulting from the activation of VTA dopaminergic neurons reverses evoked allodynia in mice with neuropathic or cancer pain without increasing threshold responses to physiological pain in sham-operated animals.

Materials and methods

Animals

The present study was conducted in accordance with the Guiding Principles for the Care and Use of Laboratory Animals, Hoshi University, as adopted by the Committee on Animal Research of Hoshi University. Male C57BL/6J mice (8–12 weeks) (Tokyo Laboratory Animals Science Co., Ltd., Tokyo, Japan) and TH-cre (B6.Cg-Tg (Th-cre) 1Tmd/J) mice (Jackson Laboratory, ME, USA) were used in this study. All mice were housed up to six mice per cage and kept in a temperature- and humidity-controlled room ($24 \pm 1^\circ\text{C}$, $55 \pm 5\%$ relative humidity) under a 12-h light–dark cycle (light on at 8 a.m.). Food and water were available ad libitum. Behavioral tests were performed in the light phase.

Mice were randomly selected for inclusion in each group by cage prior to baseline testing.

Neuropathic pain model

Mice were deeply anesthetized with isoflurane (3%, inhalation). We produced a partial nerve ligation model by using an 8-0 silk suture tightly ligated around approximately one-half of the diameter of the sciatic nerve in the right (ipsilateral) hind paw, as previously described.^{2,3} In sham-operated mice, the nerve was exposed but not ligated.

Electrophysiology

DiI (0.75 μL of 1%; Molecular Probes, OR, USA) was stereotactically infused into the N.Acc. (from bregma: anteroposterior (AP) +1.6 mm, mediolateral (ML) +1.8 mm, dorsoventral (DV) –4.0 mm at an angle of 10°) of sciatic nerve-ligated mice at a rate of 0.25 $\mu\text{L}/\text{min}$. One week after the operation, mice were anesthetized and perfused transcardially with ice-cold sucrose artificial cerebrospinal fluid (aCSF), which contained (in mM) 222.1 sucrose, 2.5 KCl, 1.4 NaH_2PO_4 , 1 CaCl_2 , 7 MgCl_2 , 27 NaHCO_3 , and 0.5 ascorbic acid (oxygenated with 95% O_2 and 5% CO_2). Coronal brain slices (300 μm thick) containing the VTA were prepared with a vibratome (VT 1200S; Leica, Wetzlar, Germany) in cold sucrose-aCSF. The slices were kept at room temperature for at least 1 h before recording in oxygenated standard aCSF that contained (in mM) 128 NaCl, 3 KCl, 1.25 NaH_2PO_4 , 2 CaCl_2 , 2 MgCl_2 , 24 NaHCO_3 , and 10 glucose.

Whole-cell current-clamp recordings were made only from fluorescently DiI-labeled VTA neurons that were visually identified by using an upright microscope (Eclipse FN1; Nikon, Tokyo, Japan) equipped with G2-A filters. Slices were superfused at ~ 2 ml/min with standard aCSF at 30°C – 32°C . Patch pipettes (4–6 M Ω) were pulled from borosilicate glass (Harvard App., GC150–7.5) on a pipette puller (P-97; Sutter Instruments, CA, USA) and filled with internal solution (pH 7.25 with KOH) consisting of (in mM) 120 K-glucuronate, 10 KCl, 10 creatine phosphate, 4 Mg-ATP, 0.3 $\text{Na}_2\text{-GTP}$, 0.2 EGTA, and 0.2% biocytin. Signals were obtained using a Multiclamp 700B amplifier (Molecular Devices, CA, USA), filtered at 2 kHz, digitized at 10 kHz using a Digidata, 1550 analog-to-digital converter (Molecular Devices) and stored using pClamp software (Molecular Devices). To probe intrinsic neuronal excitability, VTA neurons were injected with a 2-s current pulse at 50 pA increments ranging from 0 to 200 pA. The number of action potentials evoked by each current step was quantified. AP Action potentials amplitudes were measured from the resting membrane potential,

and Action potentials half-widths were measured at 50% of the peak. The threshold for Action potentials initiation was defined as the beginning of the upstroke of the spike. The amplitudes of afterhyperpolarizations were measured from the spike threshold to its peak. Resting membrane potentials were measured immediately after patch rupture and were not corrected for liquid junction potential. Series resistance (15–25 M Ω) and input resistance were monitored throughout each experiment.

Immunostaining after electrophysiology

Following electrophysiological recordings, slices were immediately fixed in 4% paraformaldehyde in phosphate-buffered saline. The sections were incubated in appropriate blocking solution and then incubated with primary antibodies (Table 1). After washes, the samples were treated with an appropriate secondary antibody or streptavidin conjugated with Alexa 488 or 647. The sections were mounted with ProLong Diamond Antifade Mountant with DAPI (Thermo Fisher Scientific, Inc., MA, USA). Fluorescence of immunolabeling was detected using an All-in-One microscope (BZ-X710, Keyence, Osaka, Japan).

Cell culture

Mouse osteosarcoma AXT cells were established as previously described⁴ and cultured under 5% CO₂ at 37°C in Iscove's modified Dulbecco's medium (IMDM) (Thermo Fischer Scientific, CA, USA) supplemented with 10% fetal bovine serum (FBS).

Tumor xenograft model

To establish tumor xenografts, AXT cells (1×10^6) suspended in 50 μ L of IMDM were injected into the right femoral bone marrow cavity of syngeneic C57BL/6J or TH-cre mice. Briefly, the knee joint was flexed to 90° and the distal side of the femur was exposed by incising the skin. A 23-gauge needle was inserted into the bone marrow cavity to make a small hole, into which AXT cells or medium alone were injected. All procedures were

performed under inhalational anesthesia with 3% isoflurane.

Virus preparation

We purchased pAAV-Flex-rev-ChR2 (H134R)-mCherry (ID:18916) from Addgene (MA, USA). AAV-Flex-rev-ChR2 (H134R)-mCherry (AAV-Flex-ChR2) was serotyped with AAV5 coat proteins and packaged by the viral vector core at University of Kyoto (Drs R Matsui and D Watanabe). The final viral concentration was 2×10^{13} particles/mL. These aliquots of virus were stored at -80°C until use.

Stereotaxic viral injections and cannula implantations

Stereotaxic injections were performed under isoflurane (3%) anesthesia and using small animal stereotaxic instruments (RWD Life Science, CA, USA). Virus (AAV-flex-ChR2) was bilaterally injected into the VTA (from bregma: AP -2.5 mm, ML ± 1.3 mm, DV -4.8 mm at an angle of 10°), at a rate of $0.25 \mu\text{L}/\text{min}$ for 4 min. More than two weeks after virus injection, mice expressing light-sensitive protein were implanted with an 8-mm fiber cannula (EIM-330; Eicom, Kyoto, Japan) above the VTA (from bregma: AP -2.5 mm, ML ± 1.3 mm, DV -3.8 mm at an angle of 10°) or N.Acc. (from bregma: AP $+1.4$ mm, ML ± 1.5 mm, DV -3.1 mm at an angle of 10°). To combine optical stimulation with simultaneous microdialysis in the N.Acc., an optogenetics-compatible microdialysis probe (CX-F-6-01; Eicom) inserted into a guide cannula (CXGF-6; Eicom) was implanted above the N.Acc. (from bregma: AP $+1.4$ mm, ML $+1.5$ mm, DV -3.6 mm at an angle of 10°).

Optical stimulation

Optical fibers (250 μm diameter; Lucir, Ibaraki, Japan) were placed inside the fiber cannula. These fibers were connected to a 473-nm blue laser (COME2-LB473/100; Lucir), and light pulses were generated through an electronic stimulator (Nihon Kohden, Tokyo, Japan).

Table 1. Details of antibodies used for immunohistochemistry.

Target	Conjugation	Host	Source	Catalog no.	Dilution
TH	None	Mouse	Immunostar	22941	1:4500
mCherry	None	Rabbit	Abcam	ab167453	1:1000
DAT	None	Rat	Millipore	MAB369	1:3500
Mouse IgG	Alexa488	Goat	Thermo Fisher Scientific	A32723	1:5000
Mouse IgG	Alexa647	Donkey	Molecular Probes	A-31571	1:3000
Rabbit IgG	Alexa546	Goat	Molecular Probes	A-11010	1:10,000
Rat IgG	Alexa488	Goat	Molecular Probes	A-11006	1:2000
Biotin (streptavidin)	Alexa488	None	Thermo Fisher Scientific	SI1223	1:3000

DAT: dopamine transporter; TH: tyrosine hydroxylase.

Mice expressing ChR2 and their controls were illuminated by blue light (473 nm, 30 Hz, 5 ms, 8 pulses every 5 s) for 30 min.

In vivo microdialysis and high-performance liquid chromatography

A microdialysis probe was implanted directly into the N. Acc. (AP, +1.4 mm; ML, +1.5 mm; DV, -3.6 mm; angle, 10°). The probe was continuously perfused with artificial cerebrospinal fluid (0.9 mM MgCl₂, 147.0 mM NaCl, 4.0 mM KCl, and 1.2 mM CaCl₂) at a flow rate of 1 μL/min by a syringe pump (ESP-32; Eicom). Outflow fractions were collected every 15 min. After more than two baseline fractions were collected, mice were subjected to optical stimulation. Dialysis samples were analyzed by high-performance liquid chromatography with electrical detection (HTEC-500; Eicom). Dopamine was separated by column chromatography and identified according to the retention times of a dopamine standard. The amount of dopamine was quantified by calculations using the peak area, and data are expressed as a percentage of the corresponding baseline peak area.

Thermal paw withdrawal test

A thermal stimulus generated using a thermal stimulus apparatus (Model 7360; UGO BASILE, Varese, Italy; model 33 Analgesia Meter; IITC/Life Science Instruments, CA, USA) was applied to the plantar surface of the mouse's hind paw to assess thermal paw withdrawal thresholds. The intensity of the thermal stimulus was adjusted to achieve an average baseline paw withdrawal latency of approximately 8 to 10 s in naive mice. A cut-off time of 15 s was used to prevent tissue damage. Quick hind paw movements away from the stimulus were considered to be a withdrawal response.

Immunohistochemistry

Mice were deeply anesthetized with isoflurane (3%, inhalation) and transcardially perfusion-fixed with 4% paraformaldehyde in 0.1 M phosphate buffer (pH 7.4). Coronal brain sections were postfixed and cryoprotected in 20–30 (w/v)% sucrose. Brain sections were then embedded in optimal cutting temperature compound (Tissue Tek; Sakura Fine Technical, Tokyo, Japan), and frozen sections were cut on a cryostat (CM1860 or CM1510; Leica Microsystems, Heidelberg, Germany) (8 μm). The brain sections were incubated in appropriate blocking solution and then incubated with primary antibodies (Table 1). Following washes, they were incubated with an appropriate secondary antibody conjugated with Alexa 488 or 546. The sections were mounted with Dako fluorescent mounting medium (Dako, Glostrup, Denmark). Fluorescence of immunolabeling was

detected using a light microscope (BX-61; Olympus, Tokyo, Japan) and photographed with a digital camera (CoolSNAP HQ; Olympus) or fluorescence microscope (BZ-X710; Keyence, Osaka, Japan).

Statistics

The data are presented as the mean ± S.E.M. We chose the sample size based on similar publications in the field. The statistical significance of differences between the groups was assessed by one-way or two-way analysis of variance followed by the Bonferroni multiple comparisons test or Sidak's test. All statistical analyses were performed with GraphPad Prism 5.0 (GraphPad Software). A p value of <0.05 was considered to reflect significance.

Results

Decreased excitability of mesolimbic dopamine neurons under neuropathic pain

Sciatic nerve ligation (SNL) as a model of neuropathic pain resulted in a marked decrease in the latency of ipsilateral hind paw withdrawal in response to normally non-noxious heat (i.e., thermal allodynia) (Figure 1(a)). In our previous studies, we hypothesized that nerve injury may affect the activity of the VTA-opioid-dopamine network.⁵ However, it remained unclear whether severe pain including cancer pain could negatively control the neuronal activity of the mesolimbic reward network and whether specific activation of this pathway could reverse hyperalgesia and allodynia related to neuropathic and cancer pain.

VTA dopamine neurons project to the N.Acc., prefrontal cortex, hippocampus, basolateral amygdala, and other regions that participate in the modulation of pain.^{6–8} To label VTA neurons terminating in the N. Acc., we injected DiI, a retrograde red fluorescent tracer, into the N.Acc. on the side contralateral to the SNL (Figure 1(b) to (d)). We performed patch-clamp electrophysiology for DiI-labeled neurons in the VTA to characterize the impact of SNL on dopaminergic neurons projecting to the N.Acc. We confirmed that DiI-positive neurons in the VTA were dopaminergic by colabeling for the enzyme TH (Figure 1(e)). We used patch-clamp electrophysiology in VTA slices from SNL- and sham-operated mice to investigate the intrinsic neuronal excitability of DiI-labeled neurons. In response to current injection, the number of spikes in DiI- and TH-positive neurons was significantly lower in the SNL group than in the sham group at all levels of current tested (Figure 1(f) and (g)). There were no significant differences in other electrophysiological

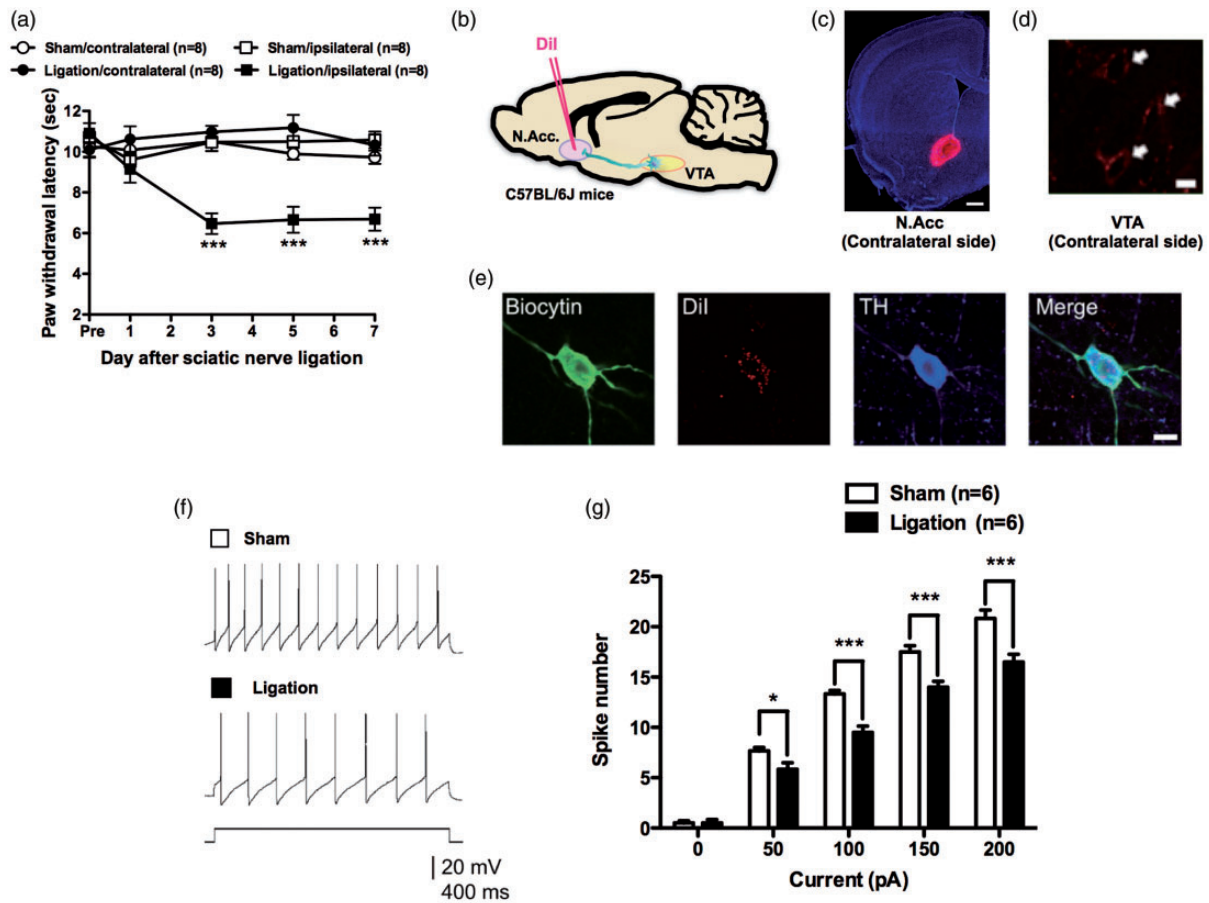


Figure 1. Sciatic nerve ligation decreases the excitability of mesolimbic dopaminergic neurons. (a) Latency of paw withdrawal in response to thermal stimulation after sham ($n = 8$) or sciatic nerve ligation ($n = 8$) (Sham-contralateral vs. Sham-ipsilateral, $F_{4,56} = 1.12$; Sham-contralateral vs. Ligation-ipsilateral, $F_{4,56} = 0.76$; Ligation-contralateral vs. Ligation-ipsilateral, $F_{4,56} = 11.13$; Sham-ipsilateral vs. Ligation-ipsilateral, $F_{4,56} = 9.98$). (b) Schematic of the experimental design. (c) DiI retrograde tracer injection site. Scale bar = $500 \mu\text{m}$. (d) DiI-labeled neurons in the VTA. Scale bar = $10 \mu\text{m}$. (e) Confocal images of biocytin-stained DiI-positive and TH-positive neurons. Scale bar = $10 \mu\text{m}$. Representative sample traces (f) and quantification of APs in response to increasing current injections (g) ($n = 6$, $F_{4,20} = 9.428$). Data are mean \pm S.E.M. * $p < 0.05$; *** $p < 0.001$; by two-way repeated measures analysis of variance (ANOVA) with a Bonferroni post hoc analysis (a) or Sidak's post hoc analysis (g).

Table 2. Electrophysiological properties of VTA dopamine neurons of sham or ligation-operated mice.

	Membrane potential (mV)	Spike threshold (mV)	Spike amplitude (mV)	Spike half-width (ms)	Spike AHP (mV)
Sham	-52.5 ± 1.4	-36.4 ± 1.2	-76.7 ± 2.0	-1.09 ± 0.07	25.9 ± 0.9
Ligation	-55.0 ± 0.9	-34.6 ± 1.3	-80.3 ± 2.5	-1.22 ± 0.05	27.7 ± 0.4

AHP: afterhyperpolarization; VTA: ventral tegmental area.

properties of VTA dopamine neurons between the two groups (Table 2).

Decreased excitability of mesolimbic dopamine neurons under cancer pain

To produce a tumor-induced bone pain model, we used severe osteosarcoma cells (AXT cells). AXT cells were established in vitro from an AX cell-derived

subcutaneous osteosarcoma, which was obtained by overexpression of *c-MYC* in bone marrow stromal cells derived from *Ink4a/Arf* ($-/-$) mice (Figure 2(a)). The intrafemoral bone marrow injection of AXT cells (Figure 2(b)) resulted in a marked decrease in the ipsilateral hind paw withdrawal latency induced by normally non-noxious heat (Figure 2(c)). To label VTA neurons terminating in the N.Acc., we injected DiI into the N.Acc. on the side contralateral to the intrafemoral bone

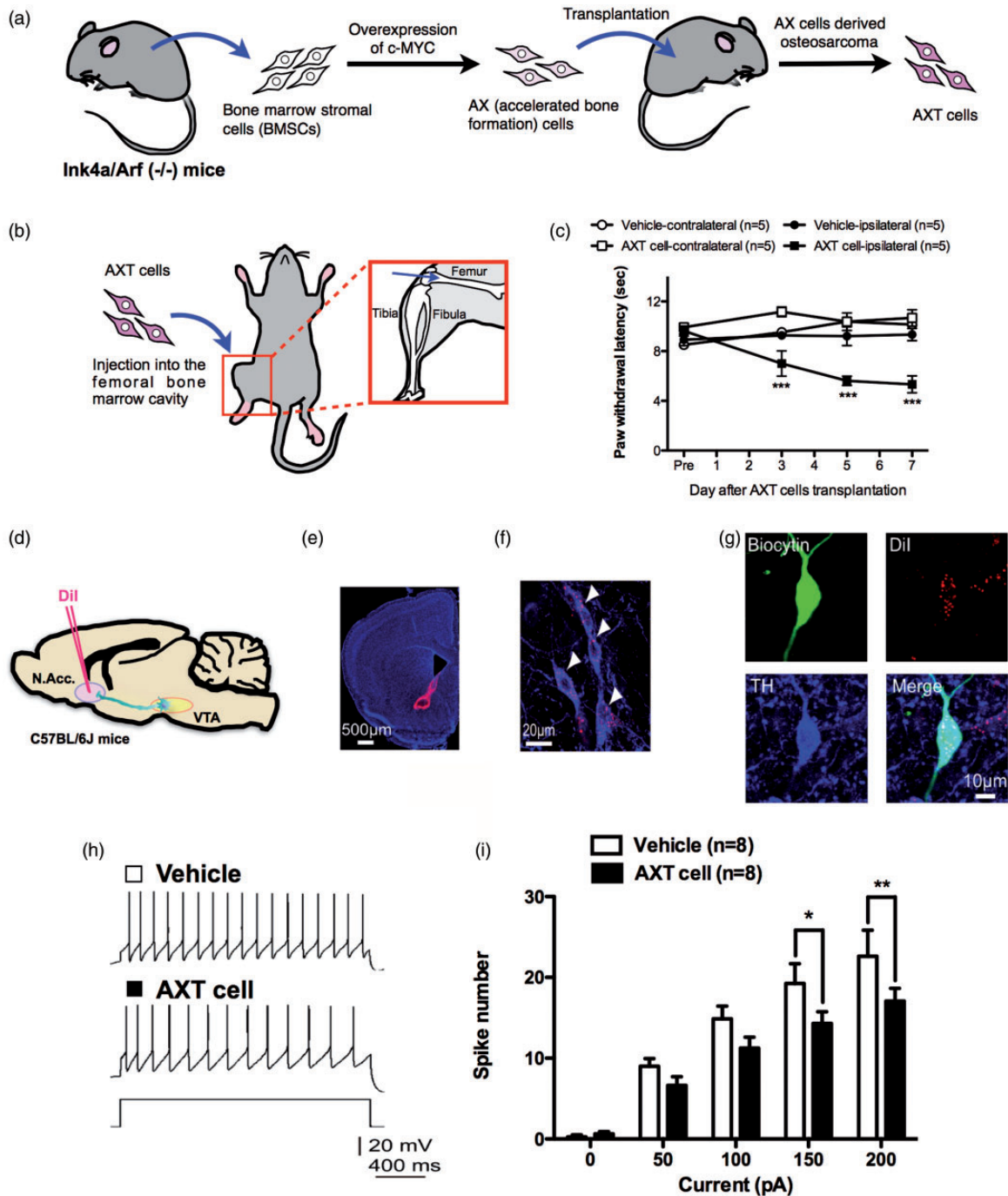


Figure 2. Cancer pain decreases the excitability of mesolimbic dopaminergic neurons. Schematic illustration of the establishment of AXT cells⁴ (a) and injection site of AXT cells (b). (c) Latency of paw withdrawal in response to thermal stimulation after vehicle (n = 5) or AXT cell transplantation (n = 5) (vehicle-contralateral vs. vehicle-ipsilateral, $F_{3,24} = 1.36$; vehicle-ipsilateral vs. AXT cell-ipsilateral, $F_{3,24} = 9.13$; AXT cell-contralateral vs. AXT cell-ipsilateral, $F_{3,24} = 10.75$). (d) Schematic of the experimental design. (e) Dil retrograde tracer injection site. Scale bar = 500 μm. (f) Dil-labeled neurons in the VTA. Scale bar = 20 μm. (g) Confocal images of biocytin-stained Dil-positive and TH-positive neurons. Scale bar = 10 μm. Representative sample traces (h) and quantification of APs in response to increasing current injections (i) (n = 8, $F_{4,28} = 2.223$). Data are mean ± S.E.M. * $p < 0.05$; ** $p < 0.01$; *** $p < 0.001$; by two-way repeated measures ANOVA with a Bonferroni post hoc analysis (c) or Sidak's post hoc analysis (i).

Table 3. Electrophysiological properties of VTA dopamine neurons of vehicle or tumor-bearing mice.

	Membrane potential (mV)	Spike threshold (mV)	Spike amplitude (mV)	Spike half-width (ms)	Spike AHP (mV)
Vehicle	-51.1 ± 1.4	-32.5 ± 1.2	-81.1 ± 2.6	-1.25 ± 0.05	27.6 ± 1.7
AxT cells	-50.2 ± 1.0	-30.9 ± 1.0	-76.2 ± 3.0	-1.37 ± 0.12	25.8 ± 2.3

AHP: afterhyperpolarization; VTA: ventral tegmental area.

marrow implantation of osteosarcoma cells (Figure 2(d) to (f)). After confirming that DiI-positive neurons in the VTA were dopaminergic by colabeling for TH (Figure 2 (g)), we used patch-clamp electrophysiology in VTA slices from tumor-bearing mice to investigate the intrinsic neuronal excitability of DiI- and TH-positive neurons. As a result, the number of spikes in DiI- and TH-positive neurons was significantly lower in the tumor-bearing group than in the control group at all levels of current tested (Figure 2(h) and (i)). There were no significant differences in other electrophysiological properties of VTA dopamine neurons between the two groups (Table 3).

Activation of mesolimbic dopamine neurons reversibly suppresses the allodynic effects of neuropathic and cancer pain

To investigate a causal link between VTA-dopamine neuron activity and thermal hyperalgesia following SNL, we generated transgenic mice expressing a light-activated nonselective cation channel, channelrhodopsin-2 (ChR2), in VTA-dopamine neurons and specifically activated VTA-dopamine neurons. TH-cre mice were injected with AAV with the FLEX switch system to express ChR2 fused with mCherry (Figure 3(a), AAV-CAG-Flex-rev-ChR2-mCherry) (TH-cre/ChR2 mice). Immunohistochemical analysis showed that ChR2-mCherry was expressed in VTA-dopamine neurons (Figure 3(b)). Next, we performed an *in vivo* microdialysis study to confirm the function of ChR2 in VTA-dopamine neurons. The dialysate dopamine levels in the N.Acc. were significantly increased by optical stimulation of the VTA in sham- and nerve-ligated mice (Figure 3(c) and (d)). Under these conditions, optical activation of VTA-dopamine neurons transiently reduced thermal hyperalgesia following SNL, but this effect was no longer evident at 2 h after optical stimulation (Figure 3(e) to (g)).

To specifically activate a mesolimbic dopaminergic pathway projecting from the VTA to the N.Acc. using optogenetics, we performed terminal stimulation in the N.Acc. of TH-cre/ChR2 mice. Immunohistochemical analysis showed that ChR2-mCherry was expressed in the N.Acc. in a subset of neurons expressing the dopamine transporter (DAT) (Figure 3(h)). Next, we performed an *in vivo* microdialysis study to confirm that

optogenetic stimulation of ChR2 in VTA-dopamine neurons terminating in the N.Acc. resulted in an increase in dialysate dopamine (Figure 3(i) and (j)). Consistent with our results regarding the optical stimulation of VTA-dopamine neurons, optical activation of terminals in the N.Acc. suppressed the allodynic effect of SNL (Figure 3(k) to (m)). Importantly, optogenetic activation of N.Acc. terminals did not produce any analgesic actions in sham-operated mice (Figure 3(e) and (m)).

In a mouse model of tumor-induced bone pain, we also investigated the effects of optical activation of VTA-dopamine neurons terminating in the N.Acc. As a result, the activation of mesolimbic dopaminergic neurons significantly suppressed the allodynia induced by intrafemoral bone marrow injection of osteosarcoma cells (Figure 4(a) to (c)).

Discussion

Chronic pain has been suggested to be associated with a hypodopaminergic state,^{9–11} a finding that is consistent with increased and decreased pain in patients with Parkinson's disease or schizophrenia, respectively.^{12–15} In addition, pain is often comorbid with other psychiatric conditions including major depressive disorder that is diagnostically characterized by anhedonia^{16,17} and increased pain sensitivity.¹⁸ Decreased tonic dopamine levels in the N.Acc. have been suggested to underlie a loss of inhibition of dopamine D2 receptor-expressing indirect pathway output neurons that may promote hypersensitivity under pain¹⁹ as well as increased impulsivity.²⁰ Ren et al. demonstrated a reduction in the spontaneous spiking of VTA dopaminergic neurons in VTA slices from mice with SNL.¹⁰ Here, we found that the firing of VTA dopamine neurons with confirmed projections to the N.Acc. was significantly decreased by SNL, consistent with observations of decreased neural activity of VTA dopamine neurons and decreased dopaminergic activation of the N.Acc. in response to a noxious stimulus in patients with chronic pain.^{21,22} We previously proposed that sustained release of β -endorphin in the VTA in the setting of sciatic nerve injury may lead to the downregulation of VTA μ -opioid receptor function, resulting in the increased activity of GABAergic μ -opioid receptor-expressing neurons and subsequently the inhibition of mesolimbic dopamine neurons.²³ Indeed, based on the molecular tagging of

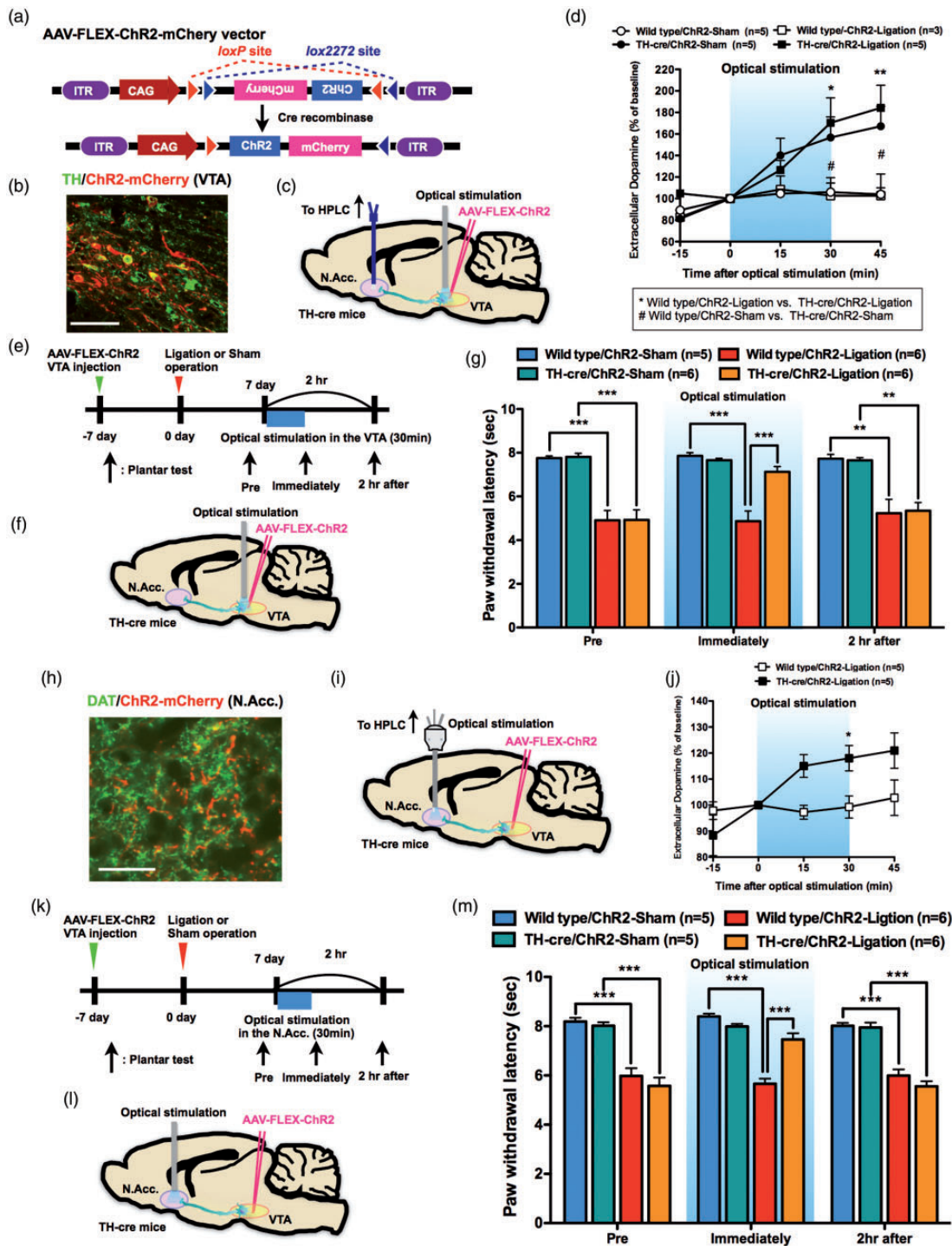


Figure 3. Activation of mesolimbic dopaminergic neurons projecting from the VTA to the N.Acc. reduces hyperalgesia following sciatic nerve ligation. (a) Construction of the Cre-dependent AAV. (b) Coexpression of ChR2-mCherry and TH. Scale bar = 50 μ m. (c) Schematic of the experimental design. (d) Extracellular dopamine levels in the N.Acc. (n = 5, Wild type/ChR2-Sham; n = 3, Wild type/ChR2-Ligation; n = 5, TH-cre/ChR2-Sham; n = 5, TH-cre/ChR2-Ligation) (Wild type/ChR2-Sham vs. Wild type/ChR2-Ligation, $F_{4,24} = 0.14$; Wild type/ChR2-Sham vs. TH-cre/ChR2-Sham, $F_{4,32} = 5.47$; Wild type/ChR2-Ligation vs. TH-cre/ChR2-Ligation, $F_{4,24} = 4.09$). (e) Experimental timeline. (f) Schematic of the experimental design. (g) Paw withdrawal latency in response to thermal stimulation (n = 5, Wild type/ChR2-Sham; n = 6, Wild type/ChR2-Ligation; n = 6, TH-cre/ChR2-Sham; n = 6, TH-cre/ChR2-Ligation). (h) Co-expression of ChR2-mCherry and DAT. Scale bar = 50 μ m. (i) Schematic of the experimental design. (j) Extracellular dopamine levels in the N.Acc. of Wild type/ChR2-Ligation mice (n = 5) and TH-cre/ChR2-Ligation mice (n = 5, $F_{4,32} = 4.28$) (k) Experimental timeline. (l) Schematic of the experimental design. (m) Paw withdrawal latency in response to thermal stimulation (n = 5, Wild type/ChR2-Sham; n = 6, Wild type/ChR2-Ligation; n = 5, TH-cre/ChR2-Sham; n = 6, TH-cre/ChR2-Ligation). Data are mean \pm S.E.M. * $p < 0.05$; ** $p < 0.01$; *** $p < 0.001$; # $p < 0.05$; by two-way repeated measures ANOVA with a Bonferroni post hoc analysis ((d) and (j)), one-way ANOVA with a Bonferroni post hoc analysis ((g) and (m)).

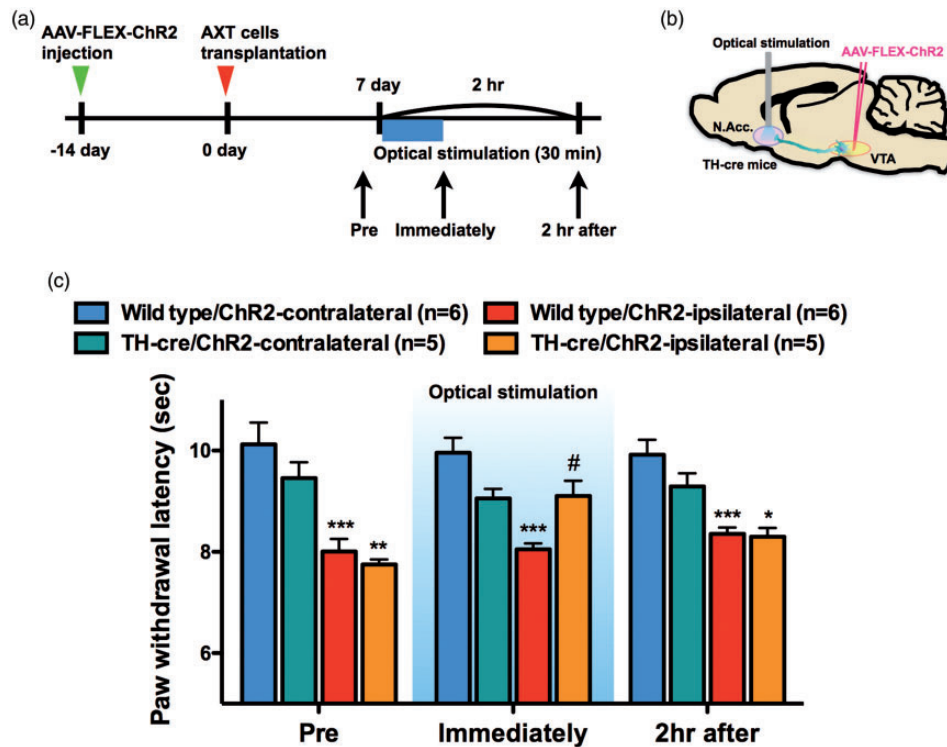


Figure 4. Activation of mesolimbic dopaminergic neurons projecting from the VTA to the N.Acc. reduces hyperalgesia following AXT cell transplantation into the femoral bone marrow cavity. (a) Experimental timeline. (b) Schematic of the experimental design. (c) Paw withdrawal latency in response to thermal stimulation ($n = 6$, Wild type/ChR2-contralateral; $n = 6$, Wild type/ChR2-ipsilateral; $n = 5$, TH-cre/ChR2-contralateral; $n = 5$, TH-cre/ChR2-ipsilateral). Data are mean \pm S.E.M. * $p < 0.05$, ** $p < 0.01$, *** $p < 0.001$, # $p < 0.05$; by one-way ANOVA with a Bonferroni post hoc analysis (c).

cFos-expressing neurons, our preliminary data suggest that neuropathic pain increases the number of activated TH-negative (putative GABAergic) neurons (unpublished observation). Taken together, these findings suggest that sustained afferent input from nerve injury may result in suppression of mesolimbic dopaminergic neurons through the activation of VTA GABA neurons.

Tumor-induced bone pain is the most common pain in patients with advanced cancer and the most common presenting symptom indicating that tumor cells have metastasized to sites beyond the primary tumor. Although the pain from bone metastases can be treated by multiple complementary approaches, bone cancer pain is still one of the most difficult of all chronic pains to fully control, since the efficacy of commonly used analgesics to treat bone cancer pain is often limited by significant adverse side effects. Little is known about the central mechanisms promoting bone cancer pain. In the present study, we found that the firing of VTA dopamine neurons with projections to the N.Acc. was significantly decreased by intrafemoral bone marrow injection of osteosarcoma cells, which produced tumor-induced bone pain. These findings suggest that tumor-induced bone pain may suppress

mesolimbic dopamine neurons, and transient activation of the mesolimbic dopamine system could reverse the tumor-induced allodynia.

The decreased activity of VTA dopaminergic cells in both the neuropathic and cancer pain models is consistent with the likelihood of decreased dopaminergic signaling in the N.Acc. and loss of inhibition of dopamine D2 receptor expressing indirect pathway neurons to promote allodynia. Our studies extend the observations of Ren et al. to reveal that targeting a subpopulation of VTA dopaminergic neurons may enable the selective modulation of allodynia associated with these chronic pain states. Importantly, our data including the sham group show that the activation of VTA dopaminergic neurons does not influence the detection of physiological thermal pain. This finding is consistent with observations in human subjects that reveal that increasing levels of dopamine pharmacologically do not result in the modulation of responses to noxious stimuli.²⁴ Thus, increased characterization of these VTA dopaminergic cells may enable selective pharmacological modulation of pathological pain, without liabilities of interfering with physiological pain or abnormal consequences of reward including addiction.

Author Contributions

MW carried out the experiments, interpreted the results, and wrote the manuscript. MN helped perform most of the experiments. YH contributed to the experiments. AY and DI contributed to the optogenetic experiments. HT carried out and analyzed the electrophysiological recordings and immunohistochemical analysis, and contributed to the manuscript. TK and TS contributed to the experiments. TS, YF, and AM contributed to the AXT cell study. HO, AY, and NK supervised the project. VLT helped to interpret the results and write the manuscript. EN and FP contributed to the discussion and helped to write the manuscript. MN supervised and conceived the project and wrote the manuscript.

Acknowledgments

The authors thank Professor Howard L Fields (University of California, San Francisco, USA) for his valuable discussions; Y Iwayama, N Uchiyama, and H Ogata for their help with the experiments; and Drs R Matsui and D Watanabe (Kyoto University) for preparing AAV-Flex-rev-ChR2-mCherry.

Declaration of Conflicting Interests

The author(s) declared no potential conflicts of interest with respect to the research, authorship, and/or publication of this article.

Funding

The author(s) disclosed receipt of the following financial support for the research, authorship, and/or publication of this article: Minoru Narita was supported by the MEXT-Supported Program for the Strategic Research Foundation at Private Universities (No. S1411019) and a JSPS Grant-in-Aid for Scientific Research (B) (No. 26293346).

References

- Fields HL. Pain: an unpleasant topic. *Pain* 1999; Suppl 6: S61–S69.
- Seltzer Z, Dubner R and Shir Y. A novel behavioral model of neuropathic pain disorders produced in rats by partial sciatic nerve injury. *Pain* 1990; 43: 205–218.
- Malmberg AB and Basbaum AI. Partial sciatic nerve injury in the mouse as a model of neuropathic pain: behavioral and neuroanatomical correlates. *Pain* 1998; 76: 215–222.
- Shimizu T, Ishikawa T, Sugihara E, et al. c-MYC over-expression with loss of Ink4a/Arf transforms bone marrow stromal cells into osteosarcoma accompanied by loss of adipogenesis. *Oncogene* 2010; 29: 5687–5699.
- Niikura K, Narita M, Nakamura A, et al. Direct evidence for the involvement of endogenous beta-endorphin in the suppression of the morphine-induced rewarding effect under a neuropathic pain-like state. *Neurosci Lett* 2008; 435: 257–262.
- Lindvall O and Björklund A. The organization of the ascending catecholamine neuron systems in the rat brain as revealed by the glyoxylic acid fluorescence method. *Acta Physiol Scand Suppl* 1974; 412: 1–48.
- Lindvall O, Björklund A, Moore RY, et al. Mesencephalic dopamine neurons projecting to neocortex. *Brain Res* 1974; 81: 325–331.
- Swanson LW. The projections of the ventral tegmental area and adjacent regions: a combined fluorescent retrograde tracer and immunofluorescence study in the rat. *Brain Res Bull* 1982; 9: 321–353.
- Ozaki S, Narita M, Iino M, et al. Suppression of the morphine-induced rewarding effect in the rat with neuropathic pain: implication of the reduction in mu-opioid receptor functions in the ventral tegmental area. *J Neurochem* 2002; 82: 1192–1198.
- Ren W, Centeno MV, Berger S, et al. The indirect pathway of the nucleus accumbens shell amplifies neuropathic pain. *Nat Neurosci* 2016; 19: 220–222.
- Loggia ML, Berna C, Kim J, et al. Disrupted brain circuitry for pain-related reward/punishment in fibromyalgia. *Arthritis Rheumatol* 2014; 66: 203–212.
- Steinberg EE and Janak PH. Establishing causality for dopamine in neural function and behavior with optogenetics. *Brain Res* 2013; 1511: 46–64.
- Stubbs B, Thompson T, Acaster S, et al. Decreased pain sensitivity among people with schizophrenia: a meta-analysis of experimental pain induction studies. *Pain* 2015; 156: 2121–2131.
- Blanchet PJ and Brefel-Courbon C. Chronic pain and pain processing in Parkinson's disease. *Prog Neuropsychopharmacol Biol Psychiatry*. Epub ahead of print 12 October 2017. DOI: 10.1016/j.pnpbp.2017.10.010.
- Maeda T, Shimo Y, Chiu SW, et al. Clinical manifestations of nonmotor symptoms in 1021 Japanese Parkinson's disease patients from 35 medical centers. *Parkinsonism Relat Disord* 2017; 38: 54–60.
- Dunlop BW and Nemeroff CB. The role of dopamine in the pathophysiology of depression. *Arch Gen Psychiatry* 2007; 64: 327–337.
- Guillin O, Abi-Dargham A and Laruelle M. Neurobiology of dopamine in schizophrenia. *Int Rev Neurobiol* 2007; 78: 1–39.
- Wojakiewicz A, Januel D, Braha S, et al. Alteration of pain recognition in schizophrenia. *Eur J Pain* 2013; 17: 1385–1392.
- Borsook D, Linnman C, Faria V, et al. Reward deficiency and anti-reward in pain chronification. *Neurosci Biobehav Rev* 2016; 68: 282–297.
- Ramdani C, Carbone L, Vidal F, et al. Dopamine precursors depletion impairs impulse control in healthy volunteers. *Psychopharmacology (Berl)* 2015; 232: 477–487.
- Baliki MN, Geha PY, Fields HL, et al. Predicting value of pain and analgesia: nucleus accumbens response to noxious stimuli changes in the presence of chronic pain. *Neuron* 2010; 66: 149–160.

22. Martikainen IK, Nuechterlein EB, Peciña M, et al. Chronic back pain is associated with alterations in dopamine neurotransmission in the ventral striatum. *J Neurosci* 2015; 35: 9957–9965.
23. Niikura K, Narita M, Butelman ER, et al. Neuropathic and chronic pain stimuli downregulate central mu-opioid and dopaminergic transmission. *Trends Pharmacol Sci* 2010; 31: 299–305.
24. Becker S, Ceko M, Louis-Foster M, et al. Dopamine and pain sensitivity: neither sulpiride nor acute phenylalanine and tyrosine depletion have effects on thermal pain sensations in healthy volunteers. *PLoS One* 2013; 8: e80766.